Journal of Pediatric Surgery (2007) **42**, 898–903

Journal of Pediatric Surgery

www.elsevier.com/locate/jpedsurg

Clinical impact of optical imaging with 3-D reconstruction of torso topography in common anterior chest wall anomalies

Philippe Poncet[b], Dragan Kravarusic[a], Tessa Richart[b], Rhiannon Evison[b], Janet L. Ronsky[b], Ali Alassiri[a], David Sigalet[a,*]

[a]*Pediatric Surgery Department, Alberta Children's Hospital, University of Calgary, Calgary, AB, Canada T2T 5C7*
[b]*Department of Mechanical and Manufacturing Engineering, University of Calgary, Calgary, AB, Canada T2N 1N4*

Index words:
Pectus excavatum;
Pectus carinatum;
Haller index;
Pectus index

Abstract

Background: Standard modalities to assist in determining the extent of chest wall developmental deformities in patients include x-ray and computed tomography (CT). The purpose of this study is to describe an optical imaging technique that provides accurate cross-sectional images of the chest, and to compare these with standard CT-derived images of chest wall abnormalities.

Patients and Methods: Ten patients (5 pectus excavatum and 5 pectus carinatum) underwent imaging that included limited CT and optical cross-sectional imaging. Severity indices of the deformity using the standard Haller index (HI) were calculated from CT scans. A similar severity measurement of deformity was derived from the outline of torso cross sections (ie, from skin to skin measurements) obtained from optical images. To assess the severity of carinatum defects, a modified pectus index was derived, which measures the anterior chest protrusion from the central chord of the chest cross section. We performed regression analyses, comparing the indices obtained from CT and optical imaging methodologies.

Results: Optical measures of cross-sectional deformities correlated well with standard HI (r^2 = 0.94) and even better with the modified pectus index (r^2 = 0.96). Adaptation of the HI for pectus carinatum deformity evaluation was effective, and consistent with the torso surface deformity measures.

Conclusions: Torso models from optical imaging offer 3-D images of the chest wall deformity with no radiation exposure. This preliminary study showed promising results for the use of torso surface measurement as an alternative index of pectus deformities; if validated in larger studies, these measures may be useful for following chest wall abnormalities, using repeated studies in patients.

Standard modalities to assist in determining the extent of chest wall development deformities in patients include x-ray and computed tomography (CT). There are several reported classification schemes; the most commonly used is the Haller index (HI) derived from CT scanning [1]. However, this requires the use of ionizing radiation, which makes repeated scanning for monitoring inadvisable. In addition, there is no validated method for the measurement of carinatum defects. The purpose of this preliminary study is to report the use of an optical imaging technique to assess

* Corresponding author. Tel.: +1 403 943 2271; fax: +1 403 943 7634.
E-mail address: sigalet@ucalgary.ca (D. Sigalet).

0022-3468/$ – see front matter © 2007 Elsevier Inc. All rights reserved.
doi:10.1016/j.jpedsurg.2006.12.070

chest wall deformities in patients with pectus excavatum and carinatum deformities.

Non-x-ray methods of detecting and monitoring musculoskeletal abnormalities (as in scoliosis) have been developed, which optically map trunk surface appearance [2-5]. Preliminary studies using optical imaging have been performed by our group using the InSpeck optical imaging system (InSpeck Inc., Montreal, Quebec, Canada) to develop a 3-dimensional surface model with superimposed texture maps of patients with chest wall deformities (Fig. 1) [6]. In preliminary work, we have shown that the optical equivalent of the HI is highly correlated with the CT equivalent. However, this does not provide a sensitive measure for the monitoring of the protrusion of carinatum defects. We have derived a modified pectus index, which measures the forward protrusion of the chest from the center chord at the widest level, as measured at the point of maximal protrusion.

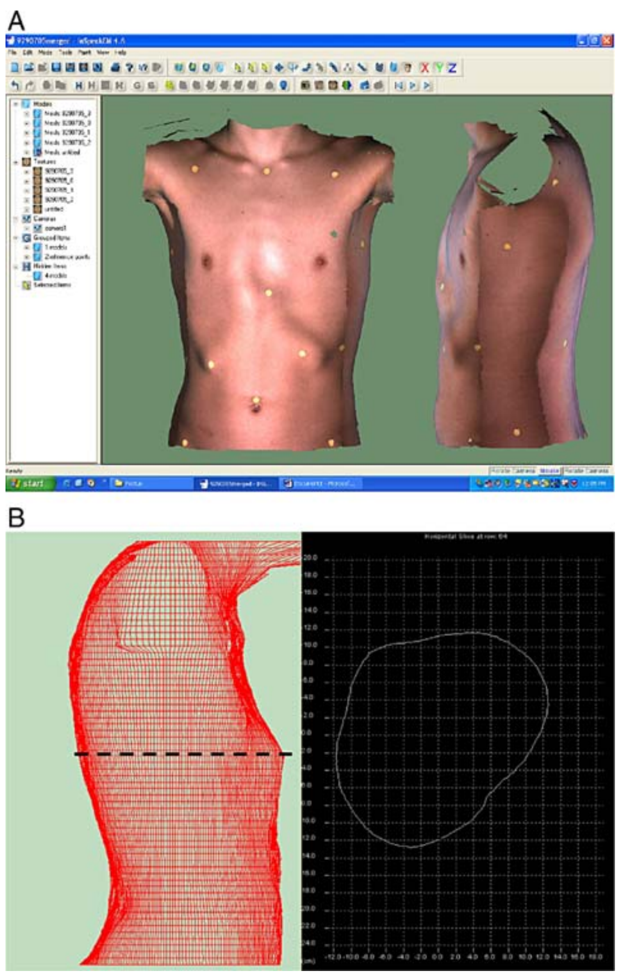

Fig. 1 Trunk surface topographies were acquired from reconstruction of the Inspeck 3D optical imaging system of a male subject showing typical pectus carinatum deformity. Three-dimensional torso models with textures before treatment, here showing (A) anterior-posterior (AP) and lateral aspects of chest wall deformities; (B) derived cross-sectional image of the trunk performed at the level where the deformity was most prominent.

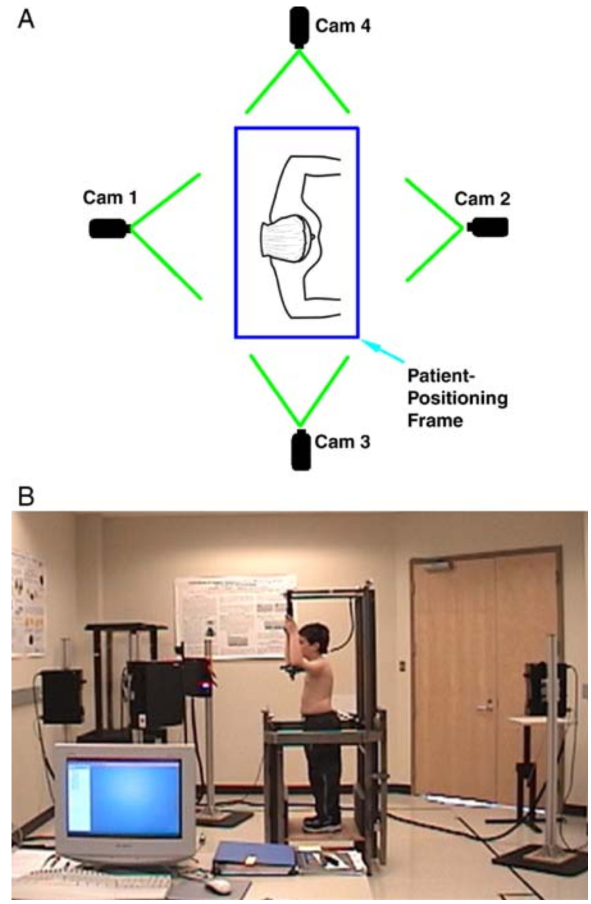

Fig. 2 (A) Schematic layout of the InSpeck system arrangement composed of 4 digitizers, allowing for a 360° contour mapping of a subject's torso. (B) A patient-positioning frame is used to stabilize the patient during the data acquisition (typically 8 seconds per full trunk digitization).

This study investigates the correlation between the Haller severity index calculated from CT scans, with the equivalent measures obtained by using a new optical imaging technology. We also studied the correlation of optical and CT-derived modified HI as a more general measurement of chest wall deformities. We hypothesized that optical imaging measures of pectus deformity would be highly correlated with the HI for pectus defects; we further hypothesized that the modified HI would be superior in measuring both excavatum and carinatum defects.

1. Method

Prospective study participants were identified from the referral base of the surgical investigator (D.L.S.). With study approval from the regional ethics review board, all patients referred for evaluation of surgical correction or bracing of chest wall defects from July 2005 to March 2006 were approached for consent after the clinic visit. All families agreed to participate; however, for logistic reasons, only patients living within 45 km of the hospital were studied.

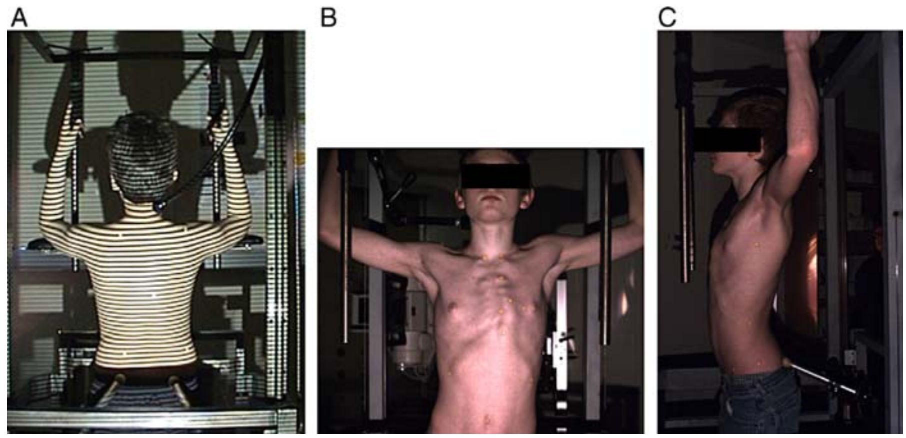

Fig. 3 (A) Structured white light technology using moiré projection images, (B) subject's positioning devices, and (C) external surface landmarks (skin markers).

Patients (n = 10) underwent imaging that included modified CT and optical imaging.

1.1. Data acquisition

All patients were interviewed at study intake, with demographic and morphologic indices collected. Each patient was asked to rate his chest wall deformity on a scale of 0 to 5, with 0 denoting that they would not ever go out in public without a shirt, with 5 being they would be comfortable with swimming in front of their peers without a shirt on (men), or in a bikini top (women).

Novel optical images were obtained by using the InSpeck system (www.inspeck.com) as modified by the Scoliosis Research Group at the Alberta Children's Hospital (ACH). This portable system comprises four 3-D

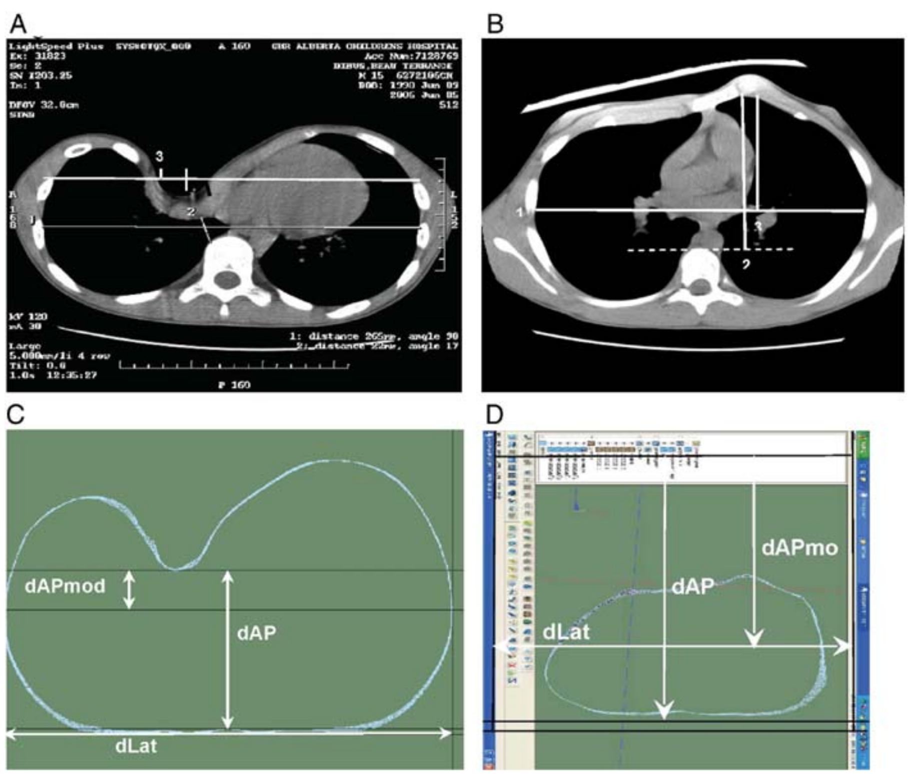

Fig. 4 Typical cross-sectional measurements of 2 subjects with pectus excavatum and carinatum defects. (A) "Classical" HI from CT: transverse diameter at the widest chord and A-P dimension from anterior vertebral body to the under surface of the sternum at the deepest point of the defect (d_{Lat}/d_{AP}). (B) "Modified" pectus index from CT: adapted for the measurement of carinatum defect: transverse diameter at the widest chord and the AP distance is measured from the central chord to the under surface of maximal excursion defect or to the under surface of maximal protrusion (d_{Lat}/d_{APmo}). Both measurements were done in all subjects. Optical measurements were done in an identical fashion (C and D), by using measurements to the external skin surface as equivalent parameters.

Table 1 Patient characteristics

No.	Age (y)	Defect type	Clinical severity (1-5)	CT index		Optical index	
				Haller index	Modified pectus index	HI	Modified pectus index
1	13	PC	4.2	1.8	2.5	1.35	1.85
2	4	PC	4.1	2.2	3.1	1.47	2.01
3	16	PC	4.2	1.7	2.6	1.22	1.78
4	13	PC	4	1.4	2.29	1.3	2.07
5	12	PC	3.0	1.19	2.27	1.07	1.33
6	14	PE	4.2	5.6	14.8	2.18	5.35
7	12	PE	4.0	3.3	6.7	1.73	3.09
8	13	PE	4.2	3.51	5.8	1.84	3.09
9	16	PE	5.0	6.0	24	2.82	11.23
10	14	PE	4.0	3.0	5.34	1.72	3.67

digitizers (Fig. 2A and B) and uses white light–diffraction interference (Fig. 3) to produce torso surface models from rapid photo exposures (0.7 s/digitizer). System accuracy, repeatability, and reliability were evaluated by using custom-designed, accurately measured (±0.006 mm) test objects (human torso replica and a trapezoidal object). Optimal digitizer orientation, lighting, calibration, image registration, and merging yielded excellent accuracies for the mannequin and the trapezoidal object (correlation coefficient $r^2 > 0.98$ mm) [7]. The new system accuracy is clearly comparable and slightly superior to other torso scanners [8].

Trunk images were obtained with each patient positioned in an alignment device with arms above shoulders (thus avoiding arm obstruction) and with 3 skin contacts (small balls) that touch at 2 points the lower back and at 1 point the base of the neck (Fig. 3A). The skin contacts minimize body sway. Small adhesive markers (Fig. 3B and C) visible in the 3-D surface images were attached to the skin at specific locations on the trunk. These markers relate internal bony structures to external surface landmarks. Three sets of trunk-surface contours (each taking less than 8 seconds) were obtained by using the optical system and data automatically recorded into a computer. Three-dimensional models (Fig. 1A) of the external surface contours of the patient's trunk with superimposed texture map were created from the surface data and used to characterize the torso surface deformities. Contours can be cut through the torso model at desired levels (Fig. 1B) and analyzed for asymmetry.

1.2. Haller index calculation

Severity indices of the deformity from CT scans using the classical HI were calculated by using standard methods [1]. In brief, the measured transverse diameter of the chest at its widest point is divided by the AP diameter at the most depressed point (as measured from the under surface of the sternum to anterior part of the vertebral body) (Fig. 4A). In the present study we have also used the HI to assess the protrusion of the carinatum defects, where the AP diameter is measured from the under surface of the sternum (point of maximal protrusion) to the front of the vertebral body (Fig. 4B). Equivalent optical surface images were obtained by using the InSpeck imaging system. Three-dimensional models of the external surface contours of the patient's torso

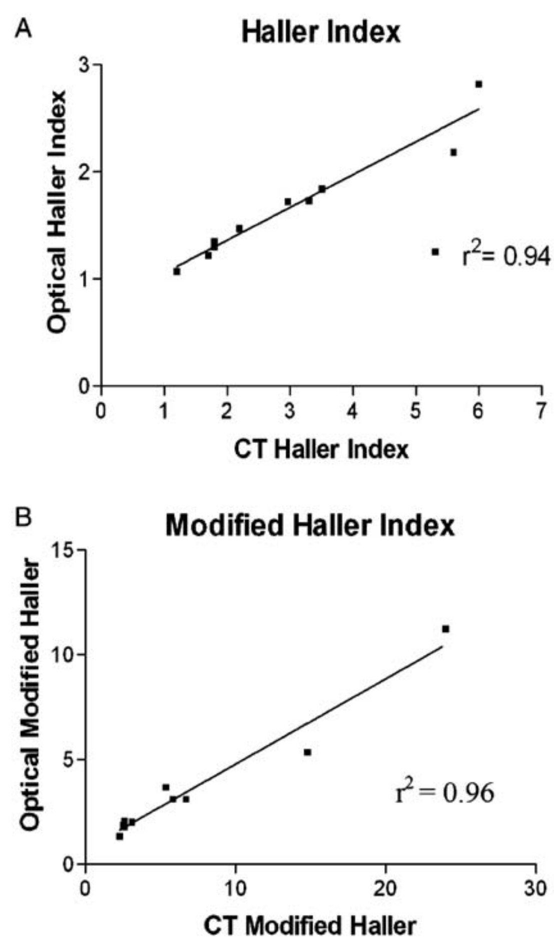

Fig. 5 Correlation of HI measurements obtained from optical images and CT scan images on the 5 excavatum and 5 carinatum pectus subjects (n = 10). (A) HI and (B) modified Pectus index.

were created from the surface data. Using the image analyzer, a cross section was cut through the torso surface model at the most sternum depressed (excavatum) or prominent (carinatum) part. Severity measurements of the deformity were derived from the outline of optical torso cross sections as the ratio of the lateral distance from left and right outer "envelope" (ie, transverse diameter from skin to skin) and AP distance measured from the posterior aspect of the vertebrae (spinous process) and the sternum deepest (excavatum) or humpiest (carinatum) deformity point on the skin surface as an equivalent to the HI obtained from CT scanning (Fig. 4C). Although the classical HI considers the front of the vertebral body in the AP diameter measurement, the equivalent index obtained from an optical cross section of torso surface reconstruction measures from the posterior part of the vertebral body (Fig. 4C) (spinous process location based on torso contour shape).

To control for this, and to provide a more sensitive measure of the anterior protrusion of carinatum defects, we devised a measurement based on the anterior projection of the chest wall from the central chord of the transverse diameter at the site of maximal protrusion (carinatum) or depression (excavatum) (Fig. 4B and D).

1.3. Statistical methods

We performed linear regression analysis between the severity measurement HI and modified HI, obtained from CT images, and the equivalent optical measurement, and computed the correlation coefficient (r^2) with Prism GraphPad Software (Prism Corp, San Francisco, Calif).

2. Results

A total of 10 patients completed the imaging protocol (Table 1). There were 5 carinatum and 5 excavatum defects. Ages, and clinical assessment of severities are presented in Table 1. Optically derived torso surface indices of deformity were consistently smaller than the standard CT indices (Table 1). Adaptation of the HI for pectus carinatum deformity evaluation was effective and consistent with the torso surface deformity measures. Torso surface indices correlated well with standard HI (r^2 = 0.94) (Fig. 5A) and correlated almost perfectly with the modified pectus index (r^2 = 0.96) (Fig. 5B).

3. Conclusion

Torso models from optical imaging offer 3-D images of the chest wall deformity with no radiation exposure. This preliminary study showed promising results for the use of torso surface measurement as an alternative to CT for the monitoring of chest wall deformities. Future work will focus on more patients and subgroups to confirm correlations and study the reliability of torso surface indices as an accurate marker of pectus deformity evaluation. In patients with scoliosis, a virtual "cut" through each vertical level produced a cross section that was often visibly asymmetric. To quantify this torso shape deformity parameters at each level were developed including the angle of back-surface rotation, rotation of principal axis, asymmetry in location and shape of left and right half-areas, and deviation of the torso centroid and spinous processes from midline [9]. Adaptation of scoliosis torso indices of transverse torso surface asymmetry may provide a valuable approach for alternative quantitative evaluation of pectus deformity and changes in chest wall deformity in braced patients.

An important advantage of this technology is the use of light images, rather than ionizing radiation. This will allow repeated studies to be performed over time, so that the effects of interventions can be more accurately followed [10]. The ability to acquire longitudinal follow-up, and with more frequent data acquisition and advanced 3-D analysis should lead to an improved understanding of the natural history of these disorders. In turn, this should improve the specificity of therapies, and, it is to be hoped, improve outcomes for these patients.

Acknowledgments

Funding for this project was from an ACH Foundation research grant, and a Canadian Institutes of Health Research operational grant. Dr Kravarusic was supported by a Remax ACH Foundation Fellowship. The helpful support of the ACH Scoliosis research team is gratefully acknowledged. As always, the expert secretarial support of Gail Wright-Wilson is very much appreciated.

References

[1] Haller Jr JA, Kramer SS, Lietman SA. Use of CT scans in selection of patients for pectus excavatum surgery: a preliminary report. J Pediatr Surg 1987;22:904-6.

[2] Liu XC, Thometz JG, Lyon RM, et al. Functional classification of patients with idiopathic scoliosis assessed by the Quantec system: a discriminant functional analysis to determine patient curve magnitude. Spine 2001;26:1274-8.

[3] Theologis TN, Fairbank JC, Turner-Smith AR, et al. Early detection of progression in adolescent idiopathic scoliosis by measurement of changes in back shape with the Integrated Shape Imaging System scanner. Spine 1997;22:1223-7.

[4] Thometz JG, Lamdan R, Liu XC, et al. Relationship between Quantec measurement and Cobb angle in patients with idiopathic scoliosis. J Pediatr Orthop 2000;20:512-6.

[5] Turner-Smith AR, Harris JD, Houghton GR, et al. A method for analysis of back shape in scoliosis. J Biomech 1988;21:497-509.

[6] Poncet P, Delorme S, Ronsky JL, et al. Reconstruction of laser-scanned 3D torso topography and stereoradiographical spine and rib-cage geometry in scoliosis. Comput Methods Biomech Biomed Engin 2000;4:59-75.

[7] Robu D, Poncet P, Cheriet F, et al. Optical imaging techniques and stereo-radiography applied in 3D reconstruction of scoliotic human

torso. Presented at the 13th Biennial Conference for Canadian Society for Biomechanics; 2004.
[8] Sciandra J, De Mauroy JC, Rolet G, et al. Accurate and fast non-contact 3-D acquisition of the whole trunk. In: D'Amico M, editor. Three-dimensional analysis of spinal deformities. Amsterdam: IOS Press; 1995. p. 81-5.
[9] Jaremko JL, Poncet P, Ronsky J, et al. Indices of torso asymmetry related to spinal deformity in scoliosis. Clin Biomech (Bristol, Avon) 2002;17:559-68.
[10] Kravarusic D, Dicken BJ, Dewar R, et al. The Calgary protocol for bracing pectus carinatum: a preliminary report. J Pediatr Surg 2006; 41:923-6.